ment 2). Because the tracks represent individual events of radionuclide decay, a Poisson distribution of tracks per cell is expected if all the cells contain an identical amount of radioisotope. Treatments 1 and 3 follow the Poisson model. The observed distribution of β tracks in treatment 2, however, differs indisputably from a Poisson distribution ($P = 10^{-7}$). There are more cells with no tracks as well as with two or three tracks than can be matched by a Poisson distribution (*10*). This finding suggests that the algal cells became labeled differentially while they were in the presence of the radioactive animals. Most cells were weakly labeled but a few apparently encountered patches enriched with $^{33}PO_4$ released by the swimming animals. Without artificial stirring the patches persisted long enough for the algal cells to exploit them. When the solution was stirred, all cells were labeled equally, indicating that the patches can be dispersed fast enough by artificial stirring to make the isotope equally available to all cells.

The results from the track autoradiography were corroborated by independent experiments in which a thin emulsion layer of Kodak NTB-2 nuclear emulsion was used and grain distributions constructed. In this case the model distribution tested is not Poisson but Neyman's type A (*11*). The distribution of tracks or grains matched that of the respective model for stirred treatments but was more skewed than the model in unstirred treatments.

The unstirred treatments we used are more representative of natural communities than the stirred treatments. When turbulent energy spectra, length scales of diffusivity, and the characteristics of fluid flow around microzooplankton are considered the prominent mechanism of dispersion in lakes and the open ocean at scales of a millimeter or less arises from molecular processes (*12*). Microcinematography has shown that the fluid environment around feeding *Daphnia* and both marine and freshwater copepods is viscous (*13*). Our results show that nutrient patches produced by zooplankton exist long enough for algae which encounter them to absorb more nutrient than do algae outside the patches. Using estimates of swimming speed and phosphorus release for *Daphnia* (*14*), we calculated characteristics of the nutrient micropatches produced by the animals. As judged by their uptake physiology, the *Chlamydomonas* can augment their cell quota by as much as 12 percent per encounter. Such circumstances place a premium on the maximal rates at which cells can sequester the enriched nutrient rather than on the efficiency with which they can gather the nutrient when ambient values are low. An important force structuring species composition in phytoplankton communities when planktonic herbivores are abundant may not be merely differential mortality imposed by the herbivores but also differential abilities of the algae to exploit short-lived nutrient patches that are rare but dependable.

JOHN T. LEHMAN
Division of Biological Sciences and
Great Lakes Research Division,
University of Michigan,
Ann Arbor 48109

DONALD SCAVIA
National Oceanic and Atmospheric Administration, Great Lakes Environmental Research Laboratory,
Ann Arbor 48104, and
Division of Biological Sciences,
University of Michigan

References and Notes

1. R. C. Dugdale, *Limnol. Oceanogr.* **12**, 685 (1967); R. W. Eppley, J. N. Rogers, J. J. McCarthy, *ibid.* **14**, 912 (1969); D. Tilman, *Science* **192**, 463 (1976).
2. P. Kilham and D. Tilman, *Ergeb. Limnol.* **13**, 110 (1979); G.-Y. Rhee and I. J. Gotham, *J. Phycol.* **16**, 486 (1980).
3. F. H. Rigler, *Limnol. Oceanogr.* **13**, 7 (1968); D. R. S. Lean, *Science* **179**, 678 (1973); J. J. McCarthy and J. C. Goldman, *ibid.* **203**, 670 (1979).
4. D. H. Turpin and P. J. Harrison, *J. Exp. Mar. Biol. Ecol.* **39**, 151 (1979); D. H. Turpin, J. S. Parslow, P. J. Harrison, *J. Plankton Res.* **3**, 421 (1980); *Can. J. Fish. Aquat. Sci.* **37**, 1193 (1980); D. Tilman, *Am. Nat.* **116**, 362 (1980).
5. J. C. Goldman, J. J. McCarthy, D. G. Peavey, *Nature (London)* **279**, 210 (1979).
6. G. A. Jackson, *ibid.* **284**, 439 (1980).
7. P. J. L. Williams and L. R. Muir, in *Ecohydrodynamics*, J. C. J. Nihoul, Ed. (Elsevier, New York, 1981), p. 209.
8. J. T. Lehman, in *Evolution and Ecology of Zooplankton Communities*, W. C. Kerfoot, Ed. (University Press of New England, Hanover, N.H., 1980), p. 251; D. Scavia, *J. Fish. Res. Board Can.* **36**, 1336 (1979).
9. At the end of 2 days in phosphorus-deficient medium the *Chlamydomonas* contained 2.4×10^{-9} μmole of phosphorus per cell and maximum uptake rates had increased to 9×10^{-11} μmole of phosphorus per cell per minute. The cells were 6 μm in diameter.
10. Chi-square goodness of fit tests were used to test our observed frequencies against the Poisson distribution with a mean equal to that estimated from the observations and 3 degrees of freedom. The difficulty of discerning many individual β tracks derived from any single cell of *Chlamydomonas* required that exposure times be kept short enough so that probabilities of finding more than four tracks per cell would be negligible.
11. N. L. Johnson and S. Kotz, *Discrete Distributions* (Houghton Mifflin, Boston, 1969), p. 216. Stirred treatments conformed to Neyman's distribution ($P > .85$), but the unstirred treatment did not ($P < .012$).
12. Observed power spectra for physical and biological properties demonstrate that the effects of large-scale physical forces dissipate effectively during the cascade to scales on the order of meters [T. M. Powell, P. J. Richerson, T. M. Dillon, B. A. Agee, B. J. Dozier, D. A. Godden, L. O. Myrup, *Science* **189**, 1088 (1975); K. L. Denman and T. Platt, *J. Mar. Res.* **34**, 593 (1976)]. Temperature microstructure in open waters suggests that diffusive fluxes at scales of centimeters are low [M. C. Gregg, C. S. Cox, P. W. Hacker, *J. Phys. Oceanogr.* **3**, 458 (1973), M. C. Gregg, *ibid.* **10**, 915 (1980)]. Thus energy at large scales is not expected to result in turbulence on scales of millimeters. Turbulence is also not likely to be generated at that scale by swimming microzooplankton because flow will be laminar, as suggested by the low Reynolds numbers (< 100) [W. C. Kerfoot, D. C. Kellog, J. R. Strickler, in *Evolution and Ecology of Zooplankton Communities*, W. C. Kerfoot, Ed. (University Press of New England, Hanover, N.H., 1980), p. 10] and by drag characteristics [J. T. Lehman, *Limnol. Oceanogr.* **22**, 170 (1977)].
13. M. Alcaraz, G.-A. Paffenhöfer, J. R. Strickler, in *Evolution and Ecology of Zooplankton Communities*, W. C. Kerfoot, Ed. (University Press of New England, Hanover, N.H., 1980), p. 241.
14. J. Gerritsen, in *ibid.*, p. 52; J. T. Lehman, *Limnol. Oceanogr.* **25**, 620 (1980).
15. Supported in part by NSF grant DEB79-22143 to J.T.L. This report is Great Lakes Environmental Research Laboratory Contribution 282.

22 December 1981; revised 11 February 1982

Residual Calcium Ions Depress Activation of Calcium-Dependent Current

Abstract. *Calcium ions enter and accumulate during depolarization of some cells, activating a potassium current, $I_{K(Ca)}$, that depends on the cytoplasmic concentration of calcium ions, $[Ca]_i$. However, elevation of $[Ca]_i$ can depress $I_{K(Ca)}$ elicited by a subsequent membrane depolarization. The depression of $I_{K(Ca)}$ is ascribed here to a $[Ca]_i$-mediated inactivation of the voltage-gated calcium conductance, which causes a net reduction in calcium ions available for the activation of $I_{K(Ca)}$. This suggests that other processes dependent on gated calcium entry may also be depressed by small background elevations in cytosolic free calcium ions.*

One regulatory function of calcium ions (Ca^{2+}) entering the cell during membrane excitation is the activation of a calcium-dependent potassium channel (*1*), which carries the current $I_{K(Ca)}$. This outward current is important in a variety of neural, sensory, and neuromuscular phenomena (*2*). It helps prevent prolonged depolarization of the membrane by the calcium current, I_{Ca}, which inactivates rather slowly and incompletely (*3, 4*), and has been implicated in cyclic pacemaker activity (*5, 6*) as well as certain neuropathologies (*7*).

At a given membrane voltage, $I_{K(Ca)}$ is activated in proportion to the intracellular concentration of free Ca^{2+} (*5, 6*). However, $I_{K(Ca)}$ elicited by a depolarizing test pulse (P_2) is reduced in amplitude if the test pulse occurs after the concen-

0036-8075/82/0514-0730S01.00/0

tration of cytoplasmic calcium, $[Ca]_i$, has increased either as a result of a conditioning depolarization (P_1) or by direct injection of Ca^{2+} (*8, 9*).

This apparent paradox, that elevation of $[Ca]_i$ by prior Ca^{2+} entry depresses a calcium-dependent process, appears now to be resolved in view of evidence that entry and accumulation of Ca^{2+} leads to a $[Ca]_i$-dependent inactivation of the voltage-gated calcium conductance (*4, 10, 11*) and evidence presented herein that depression (*12*) of $I_{K(Ca)}$ by prior Ca^{2+} entry is simply an indirect result of reduced Ca^{2+} entry and accumulation during the test pulse due to the Ca^{2+}-mediated inactivation of the calcium conductance.

Voltage clamp procedures were carried out on neurons L6 and R15 of *Aplysia californica* in such a manner as to isolate $I_{K(Ca)}$ and relate this current to the calcium current, I_{Ca}, and hence to Ca^{2+} entry and accumulation. Neurons L6 and R15 exhibited similar behavior, but only data obtained from R15 are presented here. These cells exhibit an $I_{K(Ca)}$ that is strong relative to the delayed potassium current, $I_{K(V)}$, that is purely voltage-dependent. The contribution of $I_{K(V)}$ to the total current was further reduced by the iontophoretic injection of each cell prior to the experiment with tetraethylammonium ions (TEA) from TEA-bromide–filled electrodes (about 5 minutes at 0.4 to 0.5 μA with the cell clamped at −40 mV) (*13*). The cells were bathed at 13.5° ± 0.5°C in ASW (*14*), were axotomized by undercutting, and were voltage clamped by conventional two-electrode means (*4*). Holding potential (V_h) for all experiments was −40 mV, at which the early outward current was inactivated (*15*). Correction for symmetrical leakage currents was made by summing the digitally stored currents evoked by equivalent depolarizing and hyperpolarizing pulses. At the pulse intervals used, the inward currents elicited by hyperpolarization were unaffected by prior depolarization. All potentials are absolute voltages.

Voltage clamp pulses were applied to generate a simple *I-V* plot (P_1 "off" in Fig. 1A). The characteristic hump in this plot is attributed to activation of $I_{K(Ca)}$ by Ca^{2+} influx and accumulation during the test depolarization (*1*). This component sums with a monotonically rising $I_{K(V)}$. Thus, the net current plotted in Fig. 1A is the algebraic sum of I_K [that is, $I_{K(V)} + I_{K(Ca)}$] and I_{Ca}. Each P_2 voltage was presented alternately with the conditioning pulse, P_1, off and on. With P_1 on, the Ca^{2+}-dependent hump in the plot was depressed. This protocol, when repeated in 0 m*M* Ca, ASW (triangles in Fig. 1A), suppressed both I_{Ca} and $I_{K(Ca)}$, revealing the residual $I_{K(V)}$ that was inadequately blocked by the injection of TEA. $I_{K(V)}$ accounted for a significant proportion of the total current only at potentials above +50 mV, and exhibited little inactivation with P_1 on. Essentially all the outward current depression produced by P_1 occurred in $I_{K(Ca)}$.

Subtraction of $I_{K(V)}$ from ($I_K + I_{Ca}$) produced values for ($I_{K(Ca)} + I_{Ca}$) plotted in Fig. 1B. By repeating the experiment in 200 m*M* TEA, ASW (*13*), the calcium currents were partially isolated (*16, 17*), and were plotted against voltage (Fig. 1C). It is apparent that presentation of P_1 caused a depression of $I_{K(Ca)}$ (Fig. 1B) along with an inactivation of I_{Ca} (Fig. 1C). The reduction in both I_{Ca} and $I_{K(Ca)}$ during P_2 following presentation of P_1 depends on Ca^{2+} entry during P_1 and not P_1 voltage (*4, 7, 10, 11*). In contrast, any inactivation of $I_{K(V)}$ occurs independently of Ca^{2+} entry (*18*).

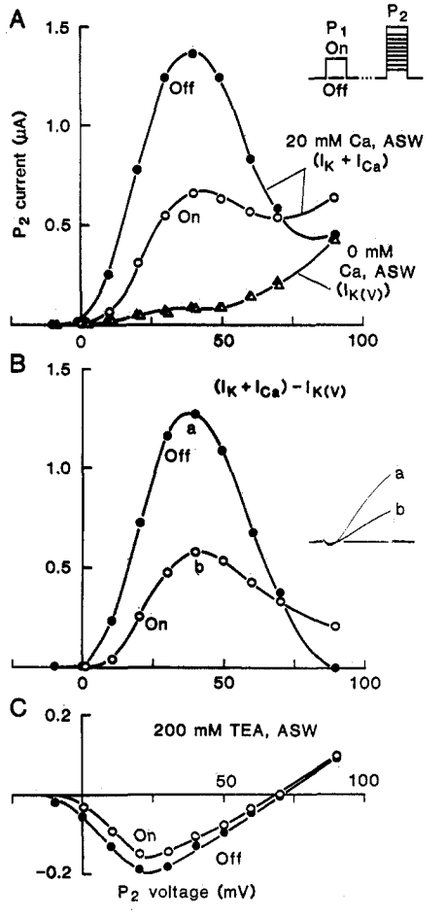

Fig. 1. Voltage relations of P_2 currents (measured at 100 msec) with P_1 "off" (closed symbols) and P_1 "on" (open symbols). (A) Cell bathed in ASW (circles) and 0 m*M* Ca, ASW (triangles). The former contains I_{Ca}, $I_{K(Ca)}$, and $I_{K(V)}$; the latter consists almost entirely of $I_{K(V)}$. Pulse 1 "on" depresses the Ca^{2+}-dependent currents selectively. (B) $I_{K(V)}$ subtracted from mixed currents in (A), leaving $I_{Ca} + I_{K(Ca)}$. The "on" plot fails to approach zero at high potentials [see (*9*)]. (C) Currents measured subsequently in 200 m*M* TEA, ASW, with subtraction of residual $I_{K(V)}$. I_{Ca} was largely inactivated and weak by this time, showing little response to P_1 "on," and considerable outward current contamination. P_1 = 200 msec, +10 mV; P_2 = 100 msec; P_1–P_2 interval = 1000 msec; pulse pairs repeated every 30 seconds; same TEA-injected neuron R15 was used throughout.

If the depression of $I_{K(Ca)}$ by prior Ca^{2+} entry is in fact simply due to reduced Ca^{2+} accumulation during the period of depolarization (t_x–t_0) accompanying reduced I_{Ca}, inactivation of I_{Ca} to differing extents should be accompanied by depression of $I_{K(Ca)}$ such that $I_{K(Ca)}$ is proportional to $\int_{t_0}^{t_x} I_{Ca}\, dt$ for short times. This reasoning is based on reports that the amplitude of $I_{K(Ca)}$ at a given voltage is linearly related to $[Ca^{2+}]_i$ (*5, 6*), and on the assumption that $[Ca^{2+}]_i$ at short times will be proportional to the time integral of I_{Ca}. The relations between $I_{K(Ca)}$ and I_{Ca} were determined as described below (*19*).

The relative contributions of $I_{K(Ca)}$ and $I_{K(V)}$ to loss of outward current during repetitive depolarization were determined by giving a train of constant-voltage pulses at 0.5 Hz to a TEA-injected cell in ASW (Fig. 2A). The early inward and the delayed outward currents both underwent progressive reduction with successful depolarizations. After replacing the ASW with 0 m*M* Ca, ASW, or 0 m*M* Ca, 20 m*M* Co, ASW, the pulses were repeated to determine $I_{K(V)}$, which was found to be less than 12 percent of the undepressed outward current recorded in ASW, and exhibited insignificant inactivation at 0.5 Hz.

The relations between $I_{K(Ca)}$ and I_{Ca} were determined by measuring the two currents in isolation, first recording the mixed currents in ASW (trace a in Fig. 2B), and then in 200 m*M* TEA, ASW (trace b), to block the remaining potassium currents and isolate I_{Ca} (*16*). I_{Ca} was then subtracted by digital means from the corresponding mixed currents recorded in ASW to yield the isolated I_K (trace a − b). This, as noted above (Fig. 2A), consisted almost exclusively of $I_{K(Ca)}$. The trajectory of $I_{K(Ca)}$ rises sigmoidally during the pulse. The slowing of its rate of rise is attributable in part to a slowing of the rate of calcium entry (trace b), and in part to a time-dependent loss of accumulated free Ca^{2+} near the inner surface of the membrane through diffusion and sequestration.

Using this method of isolating and measuring I_{Ca} and $I_{K(Ca)}$, we carried out two kinds of experiments in which the

prior entry and accumulation of Ca^{2+} was manipulated to vary the degree of inactivation of I_{Ca}. In the first, identical voltage pulses were delivered in a timed sequence, producing a progressive reduction in currents (Fig. $2C_1$). This protocol was repeated on the same cell in 200 m*M* TEA, ASW, to isolate I_{Ca} (Fig. $2C_2$) and, by subtraction of the latter, $I_{K(Ca)}$ (Fig. $2C_3$). The amplitude of $I_{K(Ca)}$ was plotted against the time integral of I_{Ca} in corresponding traces at 50, 100, and 150 msec (Fig. 2D). The relation between $I_{K(Ca)}$ measured at a given time, t_x, was a linear function of the time integral of I_{Ca}. The intercept of the regression line fell to the right of zero on the $\int_{t_0}^{t_x} I_{Ca}\, dt$ axis, the displacement increasing with increasing values of t_x (*20*).

In the other type of experiment (Fig. 2E), pulse pairs were delivered every 30 seconds, the duration of P_1 being altered so as to vary total P_1 Ca^{2+} entry. I_{Ca} and $I_{K(Ca)}$ during P_2 became smaller as the P_1 duration was increased. Again, $I_{K(Ca)}$ was a linear function of $\int_{t_0}^{t_x} I_{Ca}\, dt$ at different times, t_x, during P_2, with a similar shift of the regression lines along the abscissa with increasing values of t_x (*20*).

Since the amplitude of $I_{K(Ca)}$ rises linearly with the integral of I_{Ca} in the ranges measured, and since $I_{K(Ca)}$ is a linear function of $[Ca]_i$ (*5, 6*), the depression of $I_{K(Ca)}$ by prior Ca^{2+} entry is most simply explained as resulting from a reduced Ca^{2+} entry and accumulation during the test pulse. The elevation of $[Ca]_i$, by causing a partial inactivation of I_{Ca} (*4, 10, 11*), results in a reduced elevation of free Ca^{2+} available for the activation of $I_{K(Ca)}$ during the test depolarization. It is no longer necessary to invoke a secondary block of $I_{K(Ca)}$ by Ca^{2+} (*8, 22*) or by a Ca^{2+}-induced drop in cytoplasmic *p*H (*23*) to explain the Ca^{2+}-dependent depression of $I_{K(Ca)}$. It is also unnecessary to postulate a dual-purpose calcium-potassium channel upon which Ca^{2+} exerts both I_{Ca}-facilitating and $I_{K(Ca)}$-blocking effects (*22*).

The demonstration that elevated $[Ca]_i$ depresses $I_{K(Ca)}$ in this manner suggests that this mechanism may be involved in the regulation of other processes that depend on gated Ca^{2+} entry. Whether or not a given Ca^{2+}-dependent process lends itself to this kind of control should depend, of course, on the stoichiometry and kinetics of calcium dependency of the steps involved.

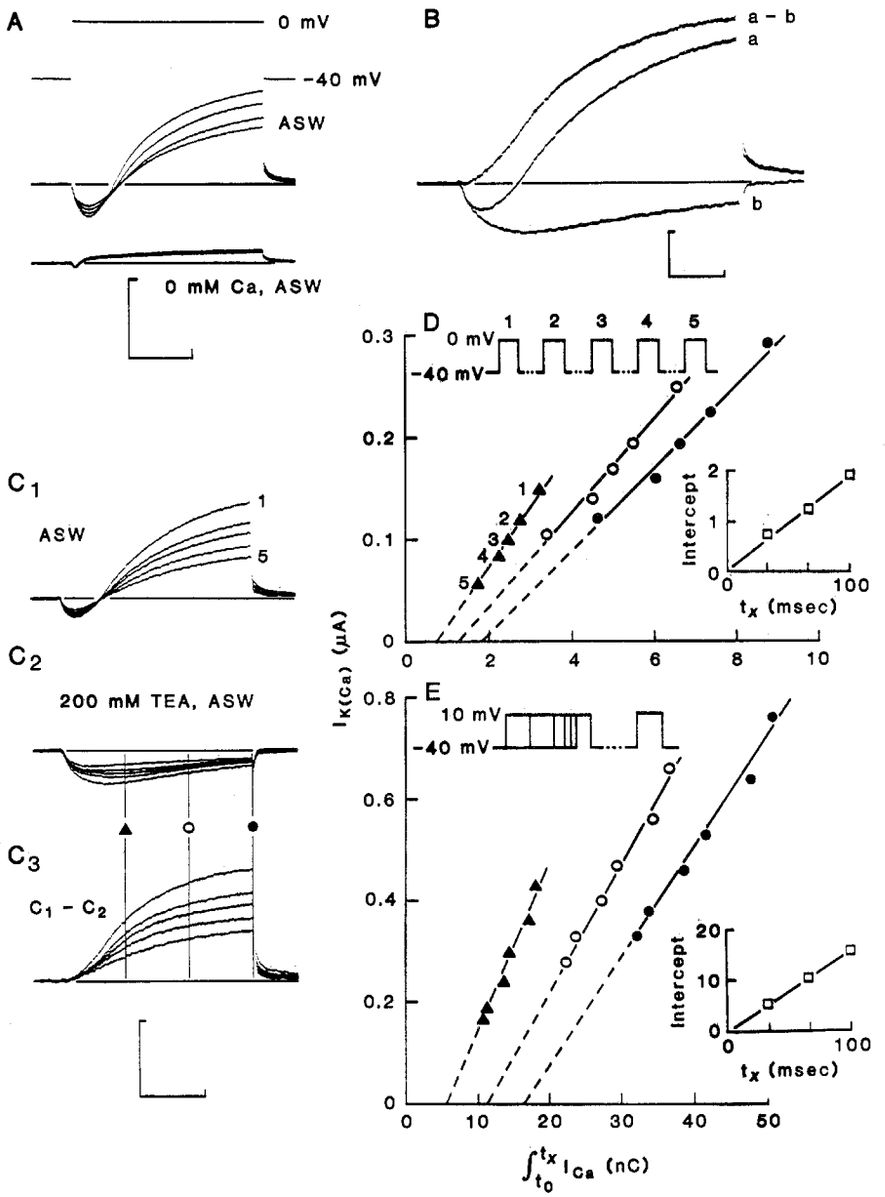

Fig. 2. Relations between $I_{K(Ca)}$ and I_{Ca}. (A) Depolarizing pulses (upper trace) delivered at 0.5 Hz produced successive loss of inward and outward currents in ASW. Sweeps 1, 2, 3, and 6 are shown (middle). Same sequence in 0 m*M* Ca, 20 m*M* Co, ASW, to determine $I_{K(V)}$ in same cell (bottom). Calibration: 0.2 μA, 50 msec. (B) Trace a, I_{Ca} + $I_{K(Ca)}$ elicited in ASW by voltage pulse to 0 mV in TEA-injected neuron R15. Trace b, I_{Ca} recorded in 200 m*M* TEA, ASW. $I_{K(Ca)}$ was determined by subtracting trace b from trace a. Calibration: 0.1 μA, 25 msec. (C_1) Currents elicited in ASW and 0 m*M* Ca, 20 m*M* Co, ASW, by 150-msec pulses to +10 mV. Pulses 1, 2, 3, 4, and 5 were separated by intervals of 4, 3, 2, and 1 second, respectively. The same procedures were used as in (B) to isolate I_{Ca} (C_2) and $I_{K(Ca)}$ (C_3). Calibration: 0.2 μA, 50 msec. (D) Same data as in (C). $I_{K(Ca)}$ measured at different times, t_x, plotted against the corresponding time integral of I_{Ca}. Values of t_x were 50 (▲), 100 (○), and 150 (●) msec as indicated in (C_2) and (C_3). Inset shows plot of *x*-axis intercepts of dashed regression lines against time of measurement, t_x. (E) Similar plot from different cell in which P_2 currents were varied by altering P_1 duration from 40 to 340 msec so as to vary P_1 Ca^{2+} entry. The P_1–P_2 interval was 850 msec throughout. Measurements were made at 50 (▲), 100 (○), and 150 (●) msec, and pulse pairs were repeated every 30 seconds.

ROGER ECKERT*
DOUGLAS EWALD
Department of Biology and *Ahmanson Laboratory of Neurobiology, University of California, Los Angeles 90024*, and *Friday Harbor Laboratories, Friday Harbor, Washington 98250*

References and Notes

1. R. W. Meech and N. B. Standen, *J. Physiol. (London)* 249, 211 (1975); W. T. Clusin, M. V. L. Bennett, *J. Gen. Physiol.* **69**, 145 (1977); R. Eckert and D. L. Tillotson, *Science* **200**, 437 (1978); A. Marty, *Nature (London)* **291**, 497 (1981); H. D. Lux, E. Neher, A. Marty, *Pflügers Arch.* **381**, 273 (1981).
2. R. W. Meech, *Symp. Soc. Exp. Biol.* **30**, 161 (1976); *Annu. Rev. Biophys. Bioeng.* **7**, 1 (1978); S. Hagiwara and L. Byerly, *Fed. Proc. Fed. Am. Soc. Exp. Biol.* **40**, 2220 (1981); *Annu. Rev. Neurosci.* **4**, 69 (1981).
3. R. Eckert and H. D. Lux, *J. Physiol. (London)* **254**, 129 (1976)
4. R. Eckert and D. L. Tillotson, *ibid.* **314**, 265 (1981).
5. A. L. F. Gorman and A. Hermann, *ibid.* **296**,

393 (1979); H. D. Lux and G. Hofmeier, *Neurosci. Lett.* **3** (Suppl.), S82 (1979); A. L. F. Gorman, A. Hermann, M. V. Thomas, *Fed. Proc. Fed. Am. Soc. Exp. Biol.* **40**, 2233 (1981).
6. A. L. F. Gorman and M. V. Thomas, *J. Physiol. (London)* **308**, 287 (1980).
7. U. Heinemann, H. D. Lux, M. J. Gutnick, *Exp. Brain Res.* **27**, 237 (1977); J. R. Hotson and D. A. Prince, *J. Neurophysiol* **43**, 409 (1980); R. A. Nicoll and B. E. Alger, *Science* **212**, 957 (1981).
8. R. Eckert and H. D. Lux, *Science* **197**, 472 (1977); C. Heyer and H. D. Lux, *J. Physiol. (London)* **262**, 349 (1976).
9. Facilitation of $I_{K(Ca)}$ can occur in place of depression under special conditions. If P_2 voltage is sufficiently high to limit calcium entry and accumulation, the residual Ca^{2+} left over at the onset of P_2 following a strong P_1 calcium entry can significantly elevate the total Ca^{2+} available for activation of $I_{K(Ca)}$ during P_2. Facilitation of $I_{K(Ca)}$ should be further enhanced under those conditions, because at high potentials the calcium-mediated inactivation of I_{Ca} is minimized [R. Eckert and D. Ewald, *Biophys. J.* **37**, 182a (1982)] whereas the calcium-dependent activation of $I_{K(Ca)}$is maximized (*5*, *6*). These arguments account for the facilitation of $I_{K(Ca)}$ seen above +75 mV in Fig. 1B, and reported for high test pulses by Gorman and Thomas (*6*).
10. P. Brehm and R. Eckert, *Science* **202**, 1203 (1978); _____, D. L. Tillotson, *J. Physiol. (London)* **306**, 193 (1980); F. M. Ashcroft and P. R. Stanfield, *Science* **213**, 224 (1981).
11. P. G. Kostyuk and O. A. Krishtal, *J. Physiol. (London)* **270**, 569 (1977); D. L. Tillotson, *Proc. Natl. Acad. Sci. U.S.A.* **76**, 1497 (1979); R. Eckert, D. L. Tillotson, P. Brehm, *Fed. Proc. Fed. Am. Soc. Exp. Biol.* **40**, 2226 (1981).
12. The term "depression" (*8*) describes the reduction in $I_{K(Ca)}$ that results from prior Ca^{2+} entry; it is not termed "inactivation" since we have no evidence that the channels carrying $I_{K(Ca)}$ are inactivated by Ca^{2+}.
13. A Hermann and A. L. F. Gorman, *Neurosci. Lett.* **12**, 87 (1979). Tetraethylammonium injection also produced some nonspecific reduction in K current which we attribute to a drop in the potassium equilibrium potential, E_K, due to a displacement of internal K^+ by TEA^+. Extracellular K^+ concentration of 20 m*M* (twice normal) further reduced E_K, and I_K, which minimized any need for series resistance correction or compensation.
14. The artificial seawater (ASW) solutions, all adjusted to *p*H 7.8 with HCl and containing 20 m*M* KCl, 0.045 m*M* tetrodotoxin, 15 m*M* tris, and 10 m*M* glucose, were made up as follows (in millimolar concentrations). ASW: 468 NaCl, 20 $CaCl_2$, 45 $MgCl_2$; 0 m*M* Ca, ASW: 468 NaCl, 65 $MgCl_2$; 0 m*M* Ca, 20 m*M* Co, ASW: 468 NaCl, 45 $MgCl_2$, 20 $CoCl_2$; 200 m*M* TEA, ASW: 268 NaCl, 20 $CaCl_2$, 45 $MgCl_2$, 200 TEA-Cl; 0 m*M* Ca, 20 m*M* Co, 200 m*M* TEA, ASW: 268 NaCl, 45 $MgCl_2$, 200 TEA-Cl, 20 $CoCl_2$.
15. S. Hagiwara and N. Saito, *J. Physiol. (London)* **148**, 161 (1959); E. Neher, *J. Gen. Physiol.* **58**, 36 (1971); A. Hermann and A. L. F. Gorman, *ibid.* **78**, 87 (1981).
16. The degree of potassium current contamination remaining in TEA depends upon membrane voltage, the residual outward current increasing as the membrane voltage becomes more positive (*13*). At +10 mV and below, the contamination of inward current by simultaneous outward current is negligible as determined from tail current measurements [R. Eckert and D. Ewald, *Biophys. J.* **33**, 145a (1981); R. Eckert, in *Mechanisms of Gated Calcium Transport Across Membranes*, S. T. Ohnishi and M. Endo, Eds. (Academic Press, New York, 1981)]. Partial correction for outward current at higher potentials was made by subtracting the outward current seen in 0 m*M* Ca, ASW. The TEA-chloride (Eastman) used in these experiments was purified [R. Zucker, *Brain Res.* **208**, 473 (1981)] to remove contaminating triethylamine.
17. The I_{Ca} was now considerably smaller and more resistant than at the beginning of the experiment, due to "run down." Residual $I_{K(V)}$ was determined by repeating the experiment in 0 m*M* Ca, 20 m*M* Co, 200 m*M* TEA, ASW, and was subtracted from I_{Ca} before the latter was plotted.
18. R. W. Aldrich, P. A. Getting, S. H. Thompson, *J. Physiol. (London)* **291**, 507 (1979).
19. In the remaining experiments all test pulses were delivered at fixed voltages below +10 mV to avoid voltage-dependent changes in activation of $I_{K(Ca)}$ (*5*, *6*, *13*), and to minimize contamination of isolated I_{Ca} by potassium currents (*16*).
20. The activation of $I_{K(Ca)}$ in response to iontophoretic injection of Ca^{2+} is linear with $[Ca]_i$ as measured with injected arsenazo III (*5*, *6*). Thus, if all the calcium carried by the Ca^{2+} current into the cell remained free, close to the membrane, and available for activation of $I_{K(Ca)}$, we would expect a relation between $I_{K(Ca)}$ and $\int I_{Ca}$ such that the regression line would pass through the origin. Since time-dependent diffusion as well as rapid sequestering of Ca^{2+} occurs after its entry into the cell (*21*), some of the Ca^{2+} should be "lost" and unavailable for activation of $I_{K(Ca)}$ as time passes. The plots and their regression-line intercepts with the $\int_{t_0}^{t_x} I_{Ca}\,dt$ axis in Fig. 2, D and E, were displaced to higher values along the axis in proportion to t_x (see insets in D and E). This suggests that there is, in fact, an increasing loss of free Ca^{2+} with time, and that the percentage of Ca^{2+} lost is greater for very weak calcium currents.
21. Z. Ahmed and J. A. Conner, *J. Physiol. (London)* **286**, 61 (1979); A. L. F. Gorman and M. V. Thomas, *ibid.* **308**, 259 (1980).
22. H. D. Lux and C. B. Heyer, in *The Neurosciences: Fourth Study Program*, F. O. Schmitt and F. G. Worden, Eds. (MIT Press, Cambridge, Mass., 1979), p. 601.
23. R. W. Meech and R. C. Thomas, *J. Physiol. (London)* **265**, 867 (1977).
24. We thank D. Junge, W. Moody, and J. Chad for helpful criticisms of an early draft, and B. Eckert for supplying specimens. Supported by PHS NS08364 and the Epilepsy Foundation of America.
* Send requests for reprints to R.E. at Department of Biology, University of California, Los Angeles 90024.

23 November 1981; revised 28 January 1982

Aircraft Monitoring of Surface Carbon Dioxide Exchange

Abstract. *Aircraft-mounted sensors were used to measure the exchange of carbon dioxide above a cornfield, a forest, and a lake under midday conditions. Mean absorption values of 3400, 1200, and 100 milligrams of carbon dioxide per square meter per hour, respectively, are consistent with reported ground-based observations of carbon dioxide flux. Such information, gathered by aircraft, could be used to provide a quantitative evaluation of source and sink distributions of carbon dioxide in the biosphere, to establish a correlation between satellite data and near-surface measurements, and to monitor crop performance.*

There is much speculation on the effects of possible changes in world climate (*1*) brought about by the rising production of CO_2 from the combustion of renewable and fossil fuels. Accurate measurements made over a period of 22 years show an increase in the atmospheric CO_2 concentration from 315 to 339 parts per million (ppm) by volume (*2*), reflecting a rate that will at least double the CO_2 concentration by the mid-21st century (*3*).

Table 1. Carbon dioxide and heat flux densities for passes over corn, forest, and water around midday on 28 August 1980.

Altitude (m)	Distance (km)	CO_2 flux density (mg m^{-2} $hour^{-1}$ $\times 10^2$)	Heat flux density (W m^{-2})
		Corn	
24	1.6	−34	42
23	1.5	−14	14
25	1.5	−35	70
33	1.6	−36	70
35	1.5	−36	63
33	1.5	−47	84
Average		−34	57
		Forest	
33	10.9	−8	56
34	10.9	−10	28
48	11.4	−11	42
47	10.5	−12	42
61	10.4	−18	56
60	10.7	−14	42
Average		−12	44
		Water	
31	3.3	−3	28
28	3.3	3	21
29	3.3	−4	14
Average		−1	21

On this basis, some climatological models predict a significant rise in the mean temperature (*4*), altered rainfall patterns, and the eventual desertification of some major food-producing regions such as the central North American Plain. Other models predict minor temperature change (*5*), better crop water use, more rapid crop development, and ultimately higher crop yields (*6*).

Although records of the oil, gas, coal, and forest industries make possible a reasonable estimate of CO_2 production, it is far more difficult to quantify the net CO_2 exchange with living biota (*7*), soils (*8*), and oceans (*9*). Thus, reliable measurements must be made over seas, forests, and cultivated and uncultivated agricultural land in order to evaluate the role of these ecosystems in the carbon cycle. Clearly, large areas are involved, and a rapid means of gathering data must be used.

To this end, we successfully used an aircraft-mounted flux-measuring system based on the eddy correlation technique to monitor CO_2 exchange over various ecosystems. This system required the continuous recording of CO_2 concentration and vertical air velocity. The aircraft, a Twin Otter, was chosen for its ability to fly at low altitudes and low speeds. Its standard instrumentation (*10*) includes a temperature sensor, a gust-probe assembly for the determination of the high-frequency component of air motion, and a Doppler radar assembly for the determination of the low-frequency component. In all, 32 parameters were recorded, 16 times per second, and all

0036-8075/82/0514-0733$01.00/0